Postcollapse dynamics of self-gravitating Brownian particles and bacterial populations

Clément Sire* and Pierre-Henri Chavanis†

*Laboratoire de Physique Théorique (FRE 2603 du CNRS), Université Paul Sabatier, 118, route de Narbonne,
31062 Toulouse Cedex 4, France*

We address the postcollapse dynamics of a self-gravitating gas of Brownian particles in D dimensions in both canonical and microcanonical ensembles. In the canonical ensemble, the postcollapse evolution is marked by the formation of a Dirac peak with increasing mass. The density profile outside the peak evolves self-similarly with decreasing central density and increasing core radius. In the microcanonical ensemble, the postcollapse regime is marked by the formation of a "binarylike" structure surrounded by an almost uniform halo with high temperature. These results are consistent with thermodynamical predictions in astrophysics. We also show that the Smoluchowski-Poisson system describing the collapse of self-gravitating Brownian particles in a strong-friction limit is isomorphic to a simplified version of the Keller-Segel equations describing the chemotactic aggregation of bacterial populations. Therefore, our study has direct applications in this biological context.

I. INTRODUCTION

Self-gravitating systems such as globular clusters and elliptical galaxies constitute a Hamiltonian system of particles in interaction that can be supposed isolated in a first approximation [1]. Since energy is conserved, the proper description of stellar systems is the microcanonical ensemble [2]. The dynamical evolution of elliptical galaxies is governed by the Vlasov-Poisson system which corresponds to a collisionless regime. On the other hand, the kinetic theory of globular clusters is based on the Landau-Poisson system (or the orbit-averaged Fokker-Planck equation) which describes a collisional evolution. These equations conserve mass and energy. Furthermore, the Landau equation increases the Boltzmann entropy (H theorem) due to stellar encounters. These equations have been studied for a long time in the astrophysical literature and a relatively good physical understanding has now been achieved [1]. In particular, globular clusters can experience core collapse [3–6] related to the "gravothermal catastrophe" concept [7].

For systems with long-range interactions, statistical ensembles are not equivalent [2]. Therefore, it is of conceptual interest to compare the microcanonical evolution of stellar systems to a canonical one in order to emphasize the analogies and differences. This can be achieved by considering a gas of self-gravitating Brownian particles [8] subject to a friction originated from the presence of an inert gas and to a stochastic force (modeling turbulent fluctuations, collisions, etc.). This system has a rigorous canonical structure where the temperature T measures the strength of the stochastic force. Thus, we can precisely check the thermodynamical predictions of Kiessling [9] and Chavanis [10] obtained in the canonical ensemble. In the mean-field approximation, the self-gravitating Brownian gas model is described by the

Kramers-Poisson system. In a strong-friction limit (or for large times) it reduces to the Smoluchowski-Poisson system. These equations conserve mass and decrease the Boltzmann free energy [11]. They possess a rich physical and mathematical structure and can lead to a situation of "isothermal collapse," which is the canonical version of the gravothermal catastrophe. These equations have not been considered by astrophysicists because the canonical ensemble is not the correct description of stellar systems and the usual astrophysical bodies do not experience friction with a gas (except dust particles in the solar nebula [12]). Yet it is clear that the self-gravitating Brownian gas model is of considerable conceptual interest in statistical mechanics to understand the strange thermodynamics of systems with long-range interactions and the inequivalence of statistical ensembles. In addition, it provides one of the first models of stochastic particles with long-range interactions, thereby extending the classical Einstein-Smoluchowski model [13] to a more general context [11].

In addition, it turns out that the same type of equations occurs in biology in relation to the chemotactic aggregation of bacterial populations [14]. A general model of chemotactic aggregation has been proposed by Keller and Segel [15] in the form of two coupled partial differential equations. In some approximation, this model reduces to the Smoluchowski-Poisson system [8]. Therefore, there exists an *isomorphism* between self-gravitating Brownian particles and bacterial colonies. Nonlocal drift-diffusion equations analogous to the Smoluchowski-Poisson system have also been introduced in two-dimensional hydrodynamics in relation to the formation of large-scale vortices such as Jupiter's great red spot [16–18]. These analogies give further physical interest to our Brownian model.

In a recent series of papers [8,19,20], we have studied the dynamics and thermodynamics of self-gravitating Brownian particles confined within a spherical box of radius R in a space of dimension D. In these works, we focused on the precollapse regime. In the canonical situation (fixed temperature T) we showed that a critical temperature T_c exists below

---

*Electronic address: Clement.Sire@irsamc.ups-tlse.fr
†Electronic address: Chavanis@irsamc.ups-tlse.fr

which the system undergoes a gravitational collapse leading to a finite-time singularity at $t=t_{coll}$. For $t \to t_{coll}$, the evolution is self-similar in the sense that the density profile evolves as $\rho(r,t)=\rho_0(t)f(r/r_0(t))$ where $f(x)$ is independent of time. For $x \to +\infty$, $f(x) \sim x^{-\alpha}$ with $\alpha=2$. The central density increases as $\rho_0 \sim (t_{coll}-t)^{-1}$ and the core radius decreases as $r_0 \sim (t_{coll}-t)^{1/\alpha}$. For $T=0$, the exponent is $\alpha=2D/(D+2)$. The scaling profiles can be calculated analytically. These results can be compared with those of Penston [21] who considered an isothermal collapse modeled by the Euler-Jeans equations. We also introduced a microcanonical description of Brownian particles by letting the temperature $T(t)$ evolve in time so as to conserve energy. This can provide a simplified model for the violent relaxation of collisionless stellar systems [17] or, simply, a numerical algorithm [11] to determine what the maximum entropy state is at fixed E and M. In the microcanonical situation, there exists a critical energy E_c (Antonov energy) below which the system collapses. For $t \to t_{coll}$, there exists a pseudoscaling regime where α passes very slowly from $\alpha_{max}=2.21\dots$ to $\alpha=2$. Numerical simulations suggest that $T(t)$ remains finite at $t=t_{coll}$ so that the true scaling regime corresponds to $\alpha=2$, as in the canonical situation [20,22].

What happens after t_{coll}? By investigating the case $T=0$, we found in [19] that the evolution continues in the postcollapse regime with the formation of a Dirac peak accreting more and more mass as $M(t) \sim (t-t_{coll})^{D/2}$ while the density outside the peak evolves self-similarly with decreasing central density $\rho_0 \sim (t-t_{coll})^{-1}$ and increasing core radius $r_0 \sim (t-t_{coll})^{(D+2)/2D}$. Our aim in this paper is to investigate the postcollapse regime for $T \neq 0$ in both canonical and microcanonical ensembles. In Sec. II, we emphasize the analogy between self-gravitating Brownian particles and bacterial populations. In the following, we shall use astrophysical terminology but we stress that our results apply equally well to biology where the chemotactic model has more concrete physical applications. In Sec. III, we set the notation and recall the main results concerning the precollapse dynamics. In Sec. IV, we study the postcollapse dynamics at $T=0$ by a method different from [19], which can be generalized at finite temperature. The postcollapse dynamics at $T>0$ is precisely considered in Sec. V. In the canonical ensemble, we show that the system forms a Dirac peak whose mass increases as $M(t) \sim (t-t_{coll})^{D/2-1}$ while the density profile for $r>0$ expands self-similarly with $\rho_0 \sim (t-t_{coll})^{-1}$ and $r_0 \sim (t-t_{coll})^{1/2}$. For large times, the system is made of a Dirac peak of mass $\sim M$ surrounded by a light gas of Brownian particles (with negligible self-interaction). Due to thermal motion, complete collapse takes an infinite time (contrary to the case $T=0$). For $t \to +\infty$, the mass contained in the Dirac peak increases as $1-M(t)/M \sim \exp(-\lambda t)$ where λ is the fundamental eigenvalue of a quantum problem. For $T \to 0$, we find that $\lambda=1/4T+c_D/T^{1/3}+\cdots$. In the microcanonical ensemble, the postcollapse regime is very pathological. The system tends to create a "Dirac peak of 0^+ mass" surrounded by a uniform halo with infinite temperature. The central structure is reminiscent of a "binary star" containing a weak mass $2m \ll M =Nm$ but a huge binding energy comparable to the potential energy of the whole cluster. Since our model is essentially a

mean-field one, the physical formation of binaries is replaced by the type of structures mentioned above. The formation of a "Dirac peak" containing the whole mass in canonical ensembles and the formation of "binaries" in microcanonical ensembles are expected from thermodynamical considerations [23,9,2,10,24,19]. These are the structures which provoke a divergence of free energy (at fixed mass and temperature) and entropy (at fixed mass and energy), respectively [19]. All these analytical results are confirmed by numerical simulations of the Smoluchowski-Poisson system in Secs. VI and VII. We were able in particular to "cross the singularity" at $t=t_{coll}$ and describe the postcollapse dynamics.

II. ANALOGY BETWEEN SELF-GRAVITATING BROWNIAN PARTICLES AND BACTERIAL POPULATIONS

A. Self-gravitating Brownian particles

We consider a system of self-gravitating Brownian particles described by the N coupled stochastic equations

$$\frac{d\mathbf{r}_i}{dt}=\mathbf{v}_i, \quad \frac{d\mathbf{v}_i}{dt}=-\xi\mathbf{v}_i-\boldsymbol{\nabla}_i U(\mathbf{r}_1,\dots,\mathbf{r}_N)+\sqrt{2D'}\mathbf{R}_i(t), \quad (1)$$

where ξ is the friction coefficient, D' is the diffusion coefficient, and $\mathbf{R}_i(t)$ is a white noise satisfying $\langle\mathbf{R}_i(t)\rangle=\mathbf{0}$ and $\langle R_{a,i}(t)R_{b,j}(t')\rangle=\delta_{ij}\delta_{ab}\delta(t-t')$, where $a,b=1,\dots,D$ refer to the coordinates of space and $i,j=1,\dots,N$ to the particles. The particles interact via the potential $U(\mathbf{r}_1,\dots,\mathbf{r}_N)=\Sigma_{i<j}u(\mathbf{r}_i-\mathbf{r}_j)$. In this paper, $u(\mathbf{r}_i-\mathbf{r}_j)$ is the Newtonian binary potential in D dimensions. The stochastic process (1) defines a *toy model* of gravitational dynamics which extends the classical Brownian model [13] to the case of stochastic particles in interaction. In this context, the friction is due to the presence of an inert gas and the stochastic force is due to classical Brownian motion, turbulence, or any other stochastic effect.

Starting from the N-body Fokker-Planck equation and using a mean-field approximation [25,26], we can derive the nonlocal Kramers equation

$$\frac{\partial f}{\partial t}+\mathbf{v}\frac{\partial f}{\partial\mathbf{r}}+\mathbf{F}\frac{\partial f}{\partial\mathbf{v}}=\frac{\partial}{\partial\mathbf{v}}\left(D'\frac{\partial f}{\partial\mathbf{v}}+\xi f\mathbf{v}\right), \quad (2)$$

where $\mathbf{F}=-\boldsymbol{\nabla}\Phi$ is the smooth gravitational force felt by the particles. The gravitational potential Φ is related to the density $\rho=\int f d^D\mathbf{v}$ by the Poisson equation

$$\Delta\Phi=S_D G\rho, \quad (3)$$

where S_D is the surface of the unit D-dimensional sphere. Equation (2) can be considered as a generalized version of the Kramers-Chandrasekhar equation introduced in a homogeneous medium [27]. In this work, the diffusion and friction model stellar encounters in a simple stochastic framework. The condition that the Maxwell-Boltzmann distribution be a stationary solution of Eq. (2) leads to the Einstein relation $\xi=D'\beta$ where $\beta=1/T$ is the inverse temperature (we have included the mass of the particles and the Boltzmann constant in the definition of T). In our case, we do *not* assume

that the medium is homogeneous, so that we have to solve the Kramers-Poisson system. This makes the study much more complicated than usual. Up to date, we do not know any astrophysical application of this model although there could be connections with the process of planetesimal formation in solar nebula [12]. Whatever, this model is interesting to develop from a conceptual point of view because it possesses a rigorous thermodynamical structure and presents the same features as more realistic models (isothermal distributions, collapse, phase transitions, etc.). For this Brownian model, the relevant ensemble is the canonical one since the temperature T is fixed. Therefore, the Kramers-Poisson system can be viewed as the canonical counterpart of the Landau-Poisson system. It is interesting to study these two models in parallel to illustrate dynamically the inequivalence of statistical ensembles for systems with long-range interactions.

To simplify the problem further, we shall consider the strong-friction limit $\xi \to +\infty$ or, equivalently, the limit of large times $t \gg \xi^{-1}$. In that approximation, we can neglect the inertia of the particles. Then, the coupled stochastic equations (1) simplify to

$$\xi \frac{d\mathbf{r}_i}{dt} = -\mathbf{\nabla}_i U(\mathbf{r}_1, \ldots, \mathbf{r}_N) + \sqrt{2D'} \mathbf{R}_i(t). \qquad (4)$$

Furthermore, to leading order, the velocity distribution is Maxwellian,

$$f(\mathbf{r}, \mathbf{v}, t) = \left(\frac{\beta}{2\pi} \right)^{D/2} \rho(\mathbf{r}, t) e^{-\beta v^2/2}, \qquad (5)$$

and the Kramers equation reduces to the Smoluchowski equation

$$\frac{\partial \rho}{\partial t} = \mathbf{\nabla} \cdot \left[\frac{1}{\xi} (T \mathbf{\nabla} \rho + \rho \mathbf{\nabla} \Phi) \right]. \qquad (6)$$

It can be shown that the Kramers equation decreases the Boltzmann free energy

$$F[f] = E - TS = \int f \frac{v^2}{2} d^D \mathbf{r} d^D \mathbf{v} + \frac{1}{2} \int \rho \Phi d^D \mathbf{r}$$
$$+ T \int f \ln f d^D \mathbf{r} d^D \mathbf{v}; \qquad (7)$$

i.e., $\dot{F} \leq 0$ and $\dot{F} = 0$ at statistical equilibrium (canonical H theorem). Similarly, the Smoluchowski equation decreases the free energy $F[\rho]$ which is obtained from $F[f]$ by using the fact that the velocity distribution is Maxwellian in the strong-friction limit. This leads to the classical expression

$$F[\rho] = T \int \rho \ln \rho \, d^D \mathbf{r} + \frac{1}{2} \int \rho \Phi \, d^D \mathbf{r}. \qquad (8)$$

The passage from the Kramers equation to the Smoluchowski equation in the strong-friction limit is classical [28]. It can also be obtained formally from a Chapman-Enskog expansion [29].

In order to prevent finite-time singularities and infinite densities, we can consider a model of self-gravitating Brownian fermions, enforcing the constraint $f \leq \eta_0$ (Pauli exclusion principle). The corresponding Kramers equation takes the form

$$\frac{\partial f}{\partial t} + \mathbf{v} \frac{\partial f}{\partial \mathbf{r}} + \mathbf{F} \frac{\partial f}{\partial \mathbf{v}} = \frac{\partial}{\partial \mathbf{v}} \left[D' \frac{\partial f}{\partial \mathbf{v}} + \xi f (\eta_0 - f) \mathbf{v} \right]. \qquad (9)$$

In the strong-friction limit, we obtain a Smoluchowski equation of the form

$$\frac{\partial \rho}{\partial t} = \mathbf{\nabla} \cdot \left[\frac{1}{\xi} (\mathbf{\nabla} p + \rho \mathbf{\nabla} \Phi) \right], \qquad (10)$$

where $p(\rho)$ is the equation of state of the Fermi gas. The fermionic Smoluchowski-Poisson system has been studied in [30]. Generalized Kramers and Smoluchowski equations are introduced in [11].

B. Keller-Segel model

The name chemotaxis refers to the motion of organisms (amoeba) induced by chemical signals (acrasin). In some cases, the biological organisms secrete a substance that has an attractive effect on the organisms themselves. Therefore, in addition to their diffusive motion, they move systematically along the gradient of concentration of the chemical they secrete (chemotactic flux). When attraction prevails over diffusion, the chemotaxis can trigger a self-accelerating process until a point at which aggregation takes place. This is the case for the slime mold *Dictyostelium Discoideum* and for the bacteria *Escherichia coli* [14].

A model of slime mold aggregation has been introduced by Keller and Segel [15] in the form of two coupled differential equations

$$\frac{\partial \rho}{\partial t} = \mathbf{\nabla} \cdot (D_2 \mathbf{\nabla} \rho) - \mathbf{\nabla} \cdot (D_1 \mathbf{\nabla} c), \qquad (11)$$

$$\frac{\partial c}{\partial t} = -k(c) c + f(c) \rho + D_c \Delta c. \qquad (12)$$

In these equations $\rho(\mathbf{r}, t)$ is the concentration of amoebae and $c(\mathbf{r}, t)$ is the concentration of acrasin. Acrasin is produced by the amoebae at a rate $f(c)$. It can also be degraded at a rate $k(c)$. Acrasin diffuse according to Fick's law with a diffusion coefficient D_c. The amoeba concentration changes as a result of an oriented chemotactic motion in the direction of a positive gradient of acrasin and a random motion analogous to diffusion. In Eq. (11), $D_2(\rho, c)$ is the diffusion coefficient of the amoebae and $D_1(\rho, c)$ is a measure of the strength of the influence of the acrasin gradient on the flow of amoebae. This chemotactic drift is the fundamental process in the problem.

A first simplification of the Keller-Segel model is provided by the system of equations

$$\frac{\partial \rho}{\partial t} = D \Delta \rho - \chi \mathbf{\nabla} \cdot (\rho \mathbf{\nabla} c), \qquad (13)$$

$$\frac{\partial c}{\partial t} = D' \Delta c + a\rho - bc, \tag{14}$$

where the parameters are positive constants. An additional simplification, introduced by Jäger and Lauckhaus [31], consists in ignoring the time derivative in Eq. (14). This is valid in the case where the diffusion coefficient D' is large. Taking also $b=0$, we obtain

$$\frac{\partial \rho}{\partial t} = D\Delta\rho - \chi \boldsymbol{\nabla} \cdot (\rho \boldsymbol{\nabla} c), \tag{15}$$

$$\Delta c = -\lambda\rho, \tag{16}$$

where $\lambda = a/D'$. Clearly, these equations are isomorphic to the Smoluchowski-Poisson system (3)–(6) describing self-gravitating Brownian particles in a strong-friction limit. In particular, the chemotactic flux plays the same role as the gravitational drift in the overdamped limit of the Brownian model. When chemotactic attraction prevails over diffusion, the system is unstable and the bacteria start to aggregate. This blowup is similar to the collapse of self-gravitating systems in a canonical situation. We note that in the Keller-Segel model, the diffusion coefficient can depend on the density, leading to anomalous diffusion. Such a situation is considered in [20] where the nonlinear Smoluchowski-Poisson system is studied.

The Keller-Segel model ignores clumping and sticking effects. However, at the late stages of the blowup, when the density of amoebae has reached high values, finite-size effects and stickiness must clearly be taken into account. As a first step, we can propose [26] to replace the classical equation (15) by an equation of the form

$$\frac{\partial \rho}{\partial t} = D\Delta\rho - \chi \boldsymbol{\nabla} \cdot [\rho(\sigma_0 - \rho) \boldsymbol{\nabla} c], \tag{17}$$

which enforces a limitation $\rho(\mathbf{r},t) < \sigma_0$ on the maximum density of amoebae. This is the counterpart of the model of self-gravitating Brownian fermions [30]. These types of nonlocal Fokker-Planck equations also occur in two-dimensional (2D) hydrodynamics and astrophysics in relation with the formation of large-scale vortices and galaxies [17,18]. Their systematic study is clearly of broad interest [11].

III. COLLAPSE DYNAMICS OF SELF-GRAVITATING BROWNIAN PARTICLES

A. Smoluchowski-Poisson system

At a given temperature T controlling the diffusion coefficient, the density $\rho(\mathbf{r},t)$ of self-gravitating Brownian particles satisfies the following coupled equations:

$$\frac{\partial \rho}{\partial t} = \boldsymbol{\nabla} \cdot \left[\frac{1}{\xi}(T \boldsymbol{\nabla} \rho + \rho \boldsymbol{\nabla} \Phi) \right], \tag{18}$$

$$\Delta\Phi = S_D G\rho, \tag{19}$$

where Φ is the gravitational potential and S_D is the surface of the unit D-dimensional sphere.

From now on, we set $M = R = G = \xi = 1$ and we restrict ourselves to spherically symmetric solutions. The equations of the problem become

$$\frac{\partial \rho}{\partial t} = \boldsymbol{\nabla} \cdot (T \boldsymbol{\nabla} \rho + \rho \boldsymbol{\nabla} \Phi), \tag{20}$$

$$\Delta\Phi = S_D\rho, \tag{21}$$

with proper boundary conditions in order to impose a vanishing particle flux on the surface of the confining sphere. These read

$$\frac{\partial \Phi}{\partial r}(0,t) = 0, \ \ \Phi(1) = \frac{1}{2-D}, \ \ T\frac{\partial \rho}{\partial r}(1) + \rho(1) = 0, \tag{22}$$

for $D > 2$. For $D=2$, we take $\Phi(1)=0$ on the boundary. Integrating Eq. (21) once, we can rewrite the Smoluchowski-Poisson system in the form of a single integro-differential equation

$$\frac{\partial \rho}{\partial t} = \frac{1}{r^{D-1}} \frac{\partial}{\partial r} \left\{ r^{D-1} \left(T\frac{\partial \rho}{\partial r} + \frac{\rho}{r^{D-1}} \int_0^r \rho(r') S_D r'^{D-1} dr' \right) \right\}. \tag{23}$$

The total energy is given as the sum of the kinetic and potential contributions:

$$E = \frac{D}{2}T + \frac{1}{2} \int \rho\Phi d^D\mathbf{r}. \tag{24}$$

The Smoluchowski-Poisson system is also equivalent to a single differential equation

$$\frac{\partial M}{\partial t} = T\left(\frac{\partial^2 M}{\partial r^2} - \frac{D-1}{r}\frac{\partial M}{\partial r} \right) + \frac{1}{r^{D-1}} M\frac{\partial M}{\partial r}, \tag{25}$$

for the quantity

$$M(r,t) = \int_0^r \rho(r') S_D r'^{D-1} dr', \tag{26}$$

which represents the mass contained within the sphere of radius r. The appropriate boundary conditions are

$$M(0,t) = N_0(t), \ \ M(1,t) = 1, \tag{27}$$

where $N_0(t)=0$, except if the density develops a condensed Dirac peak contribution at $r=0$, of total mass $N_0(t)$. It is also convenient to introduce the function $s(r,t) = M(r,t)/r^D$ satisfying

$$\frac{\partial s}{\partial t} = T\left(\frac{\partial^2 s}{\partial r^2} + \frac{D+1}{r}\frac{\partial s}{\partial r} \right) + \left(r\frac{\partial s}{\partial r} + Ds \right)s. \tag{28}$$

B. Self-similar solutions of the Smoluchowski-Poisson system

In [8,19,20], we have shown that in the canonical ensemble (fixed T), the system undergoes gravitational collapse below a critical temperature T_c depending on the dimension of space. The density develops a scaling profile, and the cen-

tral density grows and diverges at a finite time t_{coll}. The case $D=2$ was extensively studied in [19] and turns out to be very peculiar. Throughout this paper, we restrain ourselves to the more generic case $D>2$, although other dimensions play a special role as far as static properties are concerned (see [19,20]).

We look for self-similar solutions of the form

$$\rho(r,t) = \rho_0(t) f\left(\frac{r}{r_0(t)}\right), \quad r_0 = \left(\frac{T}{\rho_0}\right)^{1/2}, \quad (29)$$

where King's radius r_0 defines the size of the dense core [1]. In terms of the mass profile, we have

$$M(r,t) = M_0(t) g\left(\frac{r}{r_0(t)}\right), \quad \text{with} \quad M_0(t) = \rho_0 r_0^D, \quad (30)$$

and

$$g(x) = S_D \int_0^x f(x') x'^{D-1} dx'. \quad (31)$$

In terms of the function s, we have

$$s(r,t) = \rho_0(t) S\left(\frac{r}{r_0(t)}\right), \quad \text{with} \quad S(x) = \frac{g(x)}{x^D}. \quad (32)$$

Substituting the ansatz (32) into Eq. (28), we find that

$$\frac{d\rho_0}{dt} S(x) - \frac{\rho_0}{r_0} \frac{dr_0}{dt} x S'(x)$$
$$= \rho_0^2 \left(S''(x) + \frac{D+1}{x} S'(x) + x S(x) S'(x) + D S(x)^2 \right), \quad (33)$$

where we have set $x = r/r_0$. The variables of position and time separate provided that $\rho_0^{-2} d\rho_0/dt$ is a constant that we arbitrarily set equal to 2. After time integration, this leads to

$$\rho_0(t) = \frac{1}{2} (t_{coll} - t)^{-1}, \quad (34)$$

so that the central density becomes infinite in a finite time t_{coll}. The scaling equation now reads

$$2S + xS' = S'' + \frac{D+1}{x} S' + S(xS' + DS). \quad (35)$$

The scaling solution of Eq. (35) was obtained analytically in [19] and reads

$$S(x) = \frac{4}{D-2+x^2}, \quad (36)$$

which decays with an exponent $\alpha=2$. This leads to

$$f(x) = \frac{4(D-2)}{S_D} \frac{x^2+D}{(D-2+x^2)^2}, \quad g(x) = \frac{4x^D}{D-2+x^2}. \quad (37)$$

Note finally that within the core radius r_0, the total mass in fact vanishes as $t \to t_{coll}$. Indeed, from Eq. (30), we obtain

$$M(r_0(t),t) \sim \rho_0(t) r_0^D(t) \sim T^{D/2} (t_{coll} - t)^{D/2-1}. \quad (38)$$

Therefore, the collapse does *not* create a Dirac peak ("black hole").

In [19], we have also studied the collapse dynamics at $T=0$ for which we obtained

$$\rho_0(t) \sim S_D^{-1} (t_{coll} - t)^{-1}, \quad (39)$$

as previously, but the core radius is not given anymore by King's radius which vanishes for $T=0$. Instead, we find

$$r_0 \sim \rho_0^{-1/\alpha}, \quad (40)$$

with

$$\alpha = \frac{2D}{D+2}. \quad (41)$$

The scaling function $S(x)$ is only known implicitly:

$$\left[\frac{2}{D+2} - S(x) \right]^{D/(D+2)} = K x^{2D/(D+2)} S(x), \quad (42)$$

where K is a known constant (see [19] for details), $S(0) = 2/(D+2)$, and the large-x asymptotics $S(x) \sim f(x) \sim x^{-\alpha}$. The mass within the core radius is now

$$M(r_0(t),t) \sim \rho_0(t) r_0^D(t) \sim (t_{coll} - t)^{D/2}, \quad (43)$$

and it again tends to zero as $t \to t_{coll}$. Comparing Eqs. (38) and (43) suggests that if the temperature is very small, an apparent scaling regime corresponding to the $T=0$ case will hold up to a crossover time t_*, with

$$t_{coll} - t_* \sim T^{D/2}. \quad (44)$$

Above t_*, the $T \neq 0$ scaling ultimately prevails.

IV. POSTCOLLAPSE DYNAMICS AT $T=0$

So far, all studies concerning the collapse dynamics of self-gravitating Brownian particles have concentrated on the time period $t \lesssim t_{coll}$. A natural question arises: what is happening for $t > t_{coll}$? The first possible scenario is that the state reached at $t=t_{coll}$ is in fact a stationary state. However, it is easy to check (see [8]) that this is absolutely not the case. In addition, the preceding study leads to a sort of paradox [24]. Indeed, we know that the statistical equilibrium state in the canonical ensemble is a Dirac peak [9,10]. This is not the structure that forms at $t=t_{coll}$. This structure is singular at the origin ($\rho \sim r^{-2}$) but different from a Dirac peak (in particular the central mass is zero). This means that the evolution *must* continue after t_{coll}. In particular, we will show that the Dirac peak predicted by statistical mechanics forms in the postcollapse regime.

The scenario that we are now exploring is the following. A central Dirac peak containing a mass $N_0(t)$ emerges at $t > t_{coll}$, whereas the density for $r>0$ satisfies a scaling relation of the form

$$\rho(r,t) = \rho_0(t) f\left(\frac{r}{r_0(t)}\right), \tag{45}$$

where $\rho_0(t)$ is now decreasing with time [starting from $\rho_0(t=t_{coll}) \to +\infty$] and $r_0(t)$ grows with time [starting from $r_0(t=t_{coll})=0$]. As time increases, the residual mass for $r>0$ is progressively swallowed by the dense core made of particles which have fallen on each other. It is the purpose of the rest of this paper to show that this scenario actually holds, as well as to obtain analytical and numerical results illustrating this final collapse stage.

In this section, we present an alternative treatment to that of [19], where this scenario was analytically shown to hold at $T=0$. This new approach is a good introduction to the general $T \ne 0$ case which is studied in the next section. We refer the reader to [19] for an explicit solution of the $T=0$ post-collapse regime, which, we found, leads to a central peak containing all the mass in a finite time t_{end}.

For $T=0$, the dynamical equation for the integrated mass $M(r,t)$ reads

$$\frac{\partial M}{\partial t} = \frac{1}{r^{(D-1)}} M \frac{\partial M}{\partial r}, \tag{46}$$

with boundary conditions

$$M(0,t) = N_0(t), \quad M(1,t) = 1. \tag{47}$$

We define ρ_0 such that, for small r,

$$M(r,t) - N_0(t) = \rho_0(t) \frac{r^D}{D} + \cdots. \tag{48}$$

Up to the geometrical factor S_D^{-1}, $\rho_0(t)$ is the central residual density (the residual density is defined as the density after the central peak has been subtracted). For $r=0$, Eq. (46) leads to the evolution equation for N_0:

$$\frac{dN_0}{dt} = \rho_0 N_0. \tag{49}$$

As $N_0(t)=0$ for $t \le t_{coll}$, and since this equation is a first order differential equation, it looks like $N_0(t)$ should remain zero for $t > t_{coll}$ as well. However, since $\rho_0(t_{coll}) = +\infty$, there is mathematically speaking no global solution for this equation and nonzero values for $N_0(t)$ can emerge from Eq. (49), as will soon become clear.

We then define

$$s(r,t) = \frac{M(r,t) - N_0(t)}{r^D}, \tag{50}$$

which satisfies

$$\frac{\partial s}{\partial t} = \left(r \frac{\partial s}{\partial r} + Ds\right) s + \frac{N_0}{r^D}\left(r \frac{\partial s}{\partial r} + Ds - \rho_0\right). \tag{51}$$

By definition, we have also $s(0,t) = \rho_0(t)/D$.

We now look for a scaling solution of the form

$$s(r,t) = \rho_0(t) S\left(\frac{r}{r_0(t)}\right), \tag{52}$$

with $S(0) = D^{-1}$ and

$$\rho_0(t) = r_0(t)^{-\alpha}, \tag{53}$$

where r_0 is thus defined without ambiguity. Inserting this scaling ansatz in Eq. (51) and defining the scaling variable $x = r/r_0$, we find

$$\frac{1}{\alpha \rho_0^2} \frac{d\rho_0}{dt}(\alpha S + xS') = S(DS + xS') + \frac{N_0}{\rho_0 r_0^D} \frac{1}{x^D}(DS + xS' - 1). \tag{54}$$

Imposing scaling, we find that both time-dependent coefficients appearing in Eq. (54) should be in fact constant. We thus define a constant μ such that

$$N_0 = \mu \rho_0 r_0^D \tag{55}$$

and set

$$\frac{1}{\alpha \rho_0^2} \frac{d\rho_0}{dt} = -\kappa, \tag{56}$$

with $\kappa > 0$, as the central residual density is expected to decrease. Equation (56) implies that $\rho_0 \sim (t-t_{coll})^{-1}$, which along with Eq. (53) implies that $N_0 \sim (t-t_{coll})^{D/\alpha-1}$. We thus find a power law behavior for N_0, which, in order to be compatible with Eq. (49), leads to

$$\rho_0(t) = \left(\frac{D}{\alpha} - 1\right)(t - t_{coll})^{-1} \tag{57}$$

and then to

$$\kappa = \frac{1}{D - \alpha}. \tag{58}$$

We end up with the scaling equation

$$\frac{1}{D - \alpha}(\alpha S + xS') + S(DS + xS') + \mu x^{-D}(DS + xS' - 1) = 0. \tag{59}$$

From Eq. (59), we find that the large-x asymptotics of S is $S(x) \sim x^{-\alpha}$. In a short finite time after t_{coll}, it is clear that the large-distance behavior of the density profile ($r \gg r_0$) cannot dramatically change. We deduce that the decay of S should match the behavior for time slightly less than t_{coll} for which $S(x) \sim x^{2D/(D+2)}$. Hence the value of α should remain unchanged before and after t_{coll}. Finally, we obtain the following exact behaviors for short times after t_{coll}:

$$\rho_0(t) = \frac{D}{2}(t - t_{coll})^{-1}, \tag{60}$$

$$r_0(t) = \left(\frac{2}{D}\right)^{(D+2)/2D}(t - t_{coll})^{(D+2)/2D}, \tag{61}$$

$$N_0(t) = \mu \left(\frac{2}{D}\right)^{D/2} (t - t_{coll})^{D/2}. \tag{62}$$

We note the remarkable result that the central residual density $\rho(0,t) = S_D^{-1} \rho_0(t)$ displays a universal behavior just after t_{coll}, a result already obtained in [19]. Moreover, we find that $N_0(t)$ has the same form as the mass found within a sphere of radius $r_0(t)$ below t_{coll}, given in Eq. (43).

Moreover, the scaling function S satisfies

$$\frac{D+2}{D^2}\left(\frac{2D}{D+2}S + xS'\right) + S(DS + xS') + \mu x^{-D}(DS + xS' - 1)$$
$$= 0. \tag{63}$$

The constant μ is determined by imposing that the large-r behavior of $s(r,t)$ [or $\rho(r,t)$] exactly match (not be simply proportional) that obtained below t_{coll}, which depends on the shape of the initial condition as shown in [19]. Equation (63) can be solved implicitly by looking for solutions of the form $x^D = z[S(x)]$. After cumbersome but straightforward calculations, we obtain the implicit form

$$1 + \frac{x^D}{\mu}S(x) = \left[1 + \frac{x^D}{\mu}\left(S(x) + \frac{2}{D^2}\right)\right]^{D/(D+2)}, \tag{64}$$

which coincides with the implicit solution given in [19]. Note that $S(x)$ is a function of x^D. We check that the above result indeed leads to $S(0) = D^{-1}$ and to the large-x asymptotics

$$S(x) \sim \mu^{2/(D+2)}\left(\frac{2}{D^2}\right)^{D/(D+2)} x^{-2D/(D+2)}. \tag{65}$$

Note finally that for $T=0$, N_0 saturates to 1 in a finite time, corresponding to the deterministic collapse of the outer mass shell initially at $r=1$. Indeed, using Gauss' theorem, the position of a particle initially at $r(t=0)=1$ satisfies

$$\frac{dr}{dt} = -r^{-(D-1)}. \tag{66}$$

The position of the outer shell is then

$$r(t) = (1 - Dt)^{1/D}, \tag{67}$$

which vanishes for $t_{end} = D^{-1}$.

V. POSTCOLLAPSE DYNAMICS AT $T>0$

A. Scaling regime

In the more general case $T \neq 0$, we will proceed in a very similar way as in the previous section. We define, again,

$$s(r,t) = \frac{M(r,t) - N_0(t)}{r^D}, \tag{68}$$

where N_0 still satisfies

$$\frac{dN_0}{dt} = \rho_0 N_0. \tag{69}$$

We now obtain

$$\frac{\partial s}{\partial t} = T\left(\frac{\partial^2 s}{\partial r^2} + \frac{D+1}{r}\frac{\partial s}{\partial r}\right) + \left(r\frac{\partial s}{\partial r} + Ds\right)s$$
$$+ \frac{N_0}{r^D}\left(r\frac{\partial s}{\partial r} + Ds - \rho_0\right). \tag{70}$$

By definition, we have again $s(0,t) = \rho_0(t)/D$.

We look for a scaling solution of the form

$$s(r,t) = \rho_0(t)S\left(\frac{r}{r_0(t)}\right), \tag{71}$$

with $S(0) = D^{-1}$. As before, we define King's radius by

$$r_0 = \left(\frac{T}{\rho_0}\right)^{1/2}. \tag{72}$$

For $t < t_{coll}$, we had $s(r,t) \sim 4Tr^{-2}$ [or $S(x) \sim 4x^{-2}$]. In a very short time after t_{coll}, this property should be preserved, which implies that the postcollapse scaling function should also behave as

$$S(x) \sim 4x^{-2}, \tag{73}$$

for large x. Inserting the scaling ansatz into Eq. (70), we obtain

$$\frac{1}{2\rho_0^2}\frac{d\rho_0}{dt}(2S + xS') = S'' + \frac{D+1}{x}S' + S(DS + xS')$$
$$+ \frac{N_0}{\rho_0 r_0^D}\frac{1}{x^D}(DS + xS' - 1). \tag{74}$$

Again, this equation should be time independent for scaling to hold, which implies that there exist two constants μ and κ such that

$$N_0 = \mu \rho_0 r_0^D \tag{75}$$

and

$$\frac{1}{2\rho_0^2}\frac{d\rho_0}{dt} = -\kappa, \tag{76}$$

with $\kappa > 0$, as the central residual density is again expected to decrease. Equation (76) implies that $\rho_0 \sim (t - t_{coll})^{-1}$ and then that $N_0 \sim (t - t_{coll})^{D/2-1}$. We thus find a power law behavior for N_0, which, in order to be compatible with Eq. (69), leads to the universal behavior

$$\rho_0(t) = \left(\frac{D}{2} - 1\right)(t - t_{coll})^{-1} \tag{77}$$

and then to

$$\kappa = \frac{1}{D-2}. \tag{78}$$

We end up with the scaling equation

$$\frac{1}{D-2}(2S + xS') + S'' + \frac{D+1}{x}S' + S(DS + xS')$$
$$+ \mu x^{-D}(DS + xS' - 1) = 0, \tag{79}$$

where μ has to be chosen so that $S(x)$ satisfies the condition of Eq. (73). Its value will be determined numerically in Sec. VI for $D=3$. Note that for small x, the precollapse scaling function satisfies $S(x) - S(0) \sim x^2$, whereas the postcollapse scaling function behaves as

$$S(x) - S(0) \sim x^D. \tag{80}$$

However, contrary to the $T=0$ case, $S(x)$ is not purely a function of x^D.

Finally, we find that the weight of the central peak has a universal behavior for short time after t_{coll}:

$$N_0(t) = \mu \left(\frac{2}{D-2}\right)^{D/2-1} T^{D/2}(t - t_{coll})^{D/2-1}. \tag{81}$$

Note that $N_0(t)$ behaves in a very similar manner to the mass within a sphere of radius r_0 below t_{coll}, shown in Eq. (38). In addition, comparing Eqs. (81) and (62), we can define again a postcollapse crossover time between the $T \neq 0$ and $T=0$ regimes:

$$t_* - t_{coll} \sim T^{D/2}, \tag{82}$$

which is similar to the definition of Eq. (44).

B. Large-time limit

Contrary to the $T=0$ case, complete collapse does not take place in a finite time as thermal fluctuations always allow for some particle to escape the central strongly attractive potential. In order to illustrate this point and obtain more analytic insight into this matter, we will place ourselves in the extreme situation where almost all the mass has collapsed ($N_0 \approx 1$), and only an infinitesimal amount remains in the residual profile.

In this limit, the residual density $\rho(r,t)$ satisfies the Fokker-Planck equation

$$\frac{\partial \rho}{\partial t} = T\left(\frac{\partial^2 \rho}{\partial r^2} + \frac{D-1}{r}\frac{\partial \rho}{\partial r}\right) + \frac{1}{r^{D-1}}\frac{\partial \rho}{\partial r}, \tag{83}$$

with boundary condition

$$T\frac{\partial \rho}{\partial r}(1,t) + \rho(1,t) = 0. \tag{84}$$

The problem indeed reduces to the study of a very light gas (i.e., with negligible self-interaction) of Brownian particles submitted to the gravitational force $\mathbf{F} = -(GM/r^{D-1})\mathbf{e}_r$ of a central unit mass. Alternatively, this can also be seen as the probability distribution evolution equation of a system of two Brownian particles moving in their mutual gravitation field.

Equation (83) can be reexpressed as a Schrödinger equation (in imaginary time), thus involving a self-adjoint operator (see the Appendix). The large-time behavior is dominated by the first eigenstate. Coming back to the notation of Eq. (83), we find that

$$\rho(r,t) \sim e^{-\lambda t}\psi(r), \tag{85}$$

where ψ satisfies the eigenequation

$$-\lambda\psi(r) = T\left(\psi'' + \frac{D-1}{r}\psi'\right) + \frac{1}{r^{D-1}}\psi' \tag{86}$$

and the same boundary condition as ρ—i.e.,

$$T\psi'(1) + \psi(1) = 0. \tag{87}$$

The eigenvalue λ will also control the large-time behavior of ρ_0 and N_0 as Eqs. (69) and (85) both imply that

$$1 - N_0(t) \approx \frac{\rho_0(t)}{\lambda} \sim e^{-\lambda t}. \tag{88}$$

We did not succeed in solving analytically the above eigenequation, and for a given temperature, this has to be solved numerically. However, in the limit of very small temperature, we can apply techniques reminiscent from semiclassical analysis in quantum mechanics ($T \leftrightarrow h$). We now assume T very small and define ϕ such that

$$\psi(r) = e^{-\phi(r)/T}. \tag{89}$$

The function $h = \varphi'$ satisfies the following nonlinear first-order differential equation:

$$T\left(h' + \frac{D-1}{r}h\right) + \frac{h}{r^{D-1}} - h^2 = \lambda T, \tag{90}$$

with the simple boundary condition

$$h(1) = 1. \tag{91}$$

In the limit $T \to 0$, the term proportional to T in the left-hand side of Eq. (90) can *a priori* be discarded, leading to

$$h(r) = \frac{2\lambda T r^{D-1}}{1 + \sqrt{1 - 4\lambda T r^{2(D-1)}}}. \tag{92}$$

If $4\lambda T < 1$, the above expression is a valid perturbative solution also at $r=1$, but cannot satisfy the constraint $h(1)=1$. Hence, we conclude that in the limit of small temperature $4\lambda T \geqslant 1$, so that the above expression is only valid for r not to close to $r=1$. The above argument also suggests that λT is of order unity and we write

$$\lambda T = \frac{1}{4} + \mu^2. \tag{93}$$

To understand how the boundary condition, Eq. (91), can be in fact satisfied, one has to come back to Eq. (90), which, for $r=1$, shows that $h'(1) \sim \lambda \sim T^{-1} \gg 1$. This implies that the term Th' cannot be neglected near $r=1$ and that h varies in a noticeable way on a length scale from 1 of order T.

This suggests to define

$$z(x) = h(1 - Tx), \tag{94}$$

which satisfies (at order 0 in T)

$$-z' + z - z^2 = \frac{1}{4} + \mu^2 \tag{95}$$

and $z(0) = 1$. This equation has the unique solution

$$z(x) = \frac{1}{2} + \mu \frac{1 - 2\mu \tan(\mu x)}{2\mu + \tan(\mu x)}. \tag{96}$$

For large x, this function only has a sensible behavior for $\mu = 0$, which shows that

$$\lim_{T \to 0} \lambda T = \frac{1}{4} \tag{97}$$

and that Eq. (92) is in fact valid for $1 - r \gg (4\lambda T - 1) \to 0$. To leading order, we find

$$h(1 - Tx) \approx z_0(x) = \frac{1}{2} + \frac{1}{2 + x}. \tag{98}$$

Equations (92) and (98) show that $h(x)$ goes rapidly from 1 to $1/2$ in a small region close to $r = 1$ where h varies on the scale T. One can even compute the next correction to λT by including the next term of order T in the equation for z. Writing

$$z(x) = z_0(x) + T^{1/3} z_1(x T^{1/3}), \tag{99}$$

we find

$$z_1' + \frac{2}{u} z_1 + z_1^2 - \frac{D-1}{2} u = -\frac{\mu^2}{T^{2/3}} = -c_D, \quad u = T^{1/3} x. \tag{100}$$

This is again an eigenvalue problem which selects a unique constant c_D, which we could only solve numerically. Still, this leads to the nontrivial result

$$\lambda = \frac{1}{4T} + \frac{c_D}{T^{1/3}} + \cdots \quad (T \to 0). \tag{101}$$

We now solve the eigenvalue problem (86) and (87) in the limit of large temperatures $T \to +\infty$ (see also the Appendix). We again perform the change of variables (89) and rewrite Eq. (90) in the form

$$h' + \frac{D-1}{r} h = \lambda - \frac{1}{T} \left(\frac{h}{r^{D-1}} - h^2 \right). \tag{102}$$

Then, we expand the solutions of this equation in terms of the small parameter $1/T \ll 1$. We write $h = h_0 + (1/T)h_1 + (1/T^2)h_2 + \cdots$ and $\lambda = \lambda_0 + (1/T)\lambda_1 + (1/T^2)\lambda_2 + \cdots$. To zeroth order, we have

$$h_0' + \frac{D-1}{r} h_0 = \lambda_0. \tag{103}$$

The solution of this equation is $h_0 = \lambda_0 r/D$. Using the boundary condition $h_0(1) = 1$, we obtain

$$\lambda_0 = D, \quad h_0 = r, \tag{104}$$

and $h_n(1) = 0$ for $n > 0$. To first order, we get

$$h_1' + \frac{D-1}{r} h_1 = \lambda_1 - \frac{h_0}{r^{D-1}} + h_0^2. \tag{105}$$

Integrating this first-order differential equation and using the boundary condition $h_1(1) = 0$, we obtain

$$h_1 = \frac{D}{2(D+2)} r - \frac{1}{2} r^{3-D} + \frac{r^3}{D+2}, \tag{106}$$

with

$$\lambda_1 = \frac{D^2}{2(D+2)}. \tag{107}$$

Hence, the large-temperature behavior of the eigenvalue is

$$\lambda = D + \frac{D^2}{2(D+2)} \frac{1}{T} + \cdots \quad (T \to +\infty). \tag{108}$$

This expansion can be easily carried out to higher orders but the coefficients are more and more complicated. Restricting ourselves to $D = 3$, we get

$$\lambda = 3 + \frac{9}{10} \frac{1}{T} - \frac{477}{700} \frac{1}{T^2} + O(T^{-3}).$$

VI. NUMERICAL SIMULATIONS IN THE CANONICAL ENSEMBLE

In this section, we illustrate the analytical results obtained in the previous section in the case of $D = 3$. Except when specified otherwise, our simulations have been performed at $T = 1/5 < T_c \approx 0.397\ldots$, for which we have obtained $t_{coll} \approx 0.44408\ldots$.

In order to perform our simulations, we have used a Runge-Kutta algorithm with adaptive step in space and time. We call dr the spatial discretization near $r = 0$ (which we need to take very small as the density profile becomes singular at $r = 0$). An important numerical problem arises in the numerical integration of Eq. (69), which is crucial in obtaining nonzero values for $N_0(t)$. As this equation is a first-order differential equation with initial condition $N_0(0) = 0$, any naive integration scheme should lead to a strictly vanishing value for $N_0(t)$ for all time and any dr. Still, when performing this naive numerical integration, we see that crossing t_{coll} generates increasing values for $M(dr, t)$, although keeping $M(0, t) = N_0(t) = 0$ ultimately makes the numerical integration unstable. In order to bypass this problem, we have decided to introduce a numerical scheme where Eq. (69) is replaced by

$$\frac{dN_0}{dt} = \rho_0^{fit} N_0^{fit}. \tag{109}$$

N_0^{fit} and ρ_0^{fit} are extracted from a fit of $M(r, t)$ to the functional form (we are in $D = 3$)
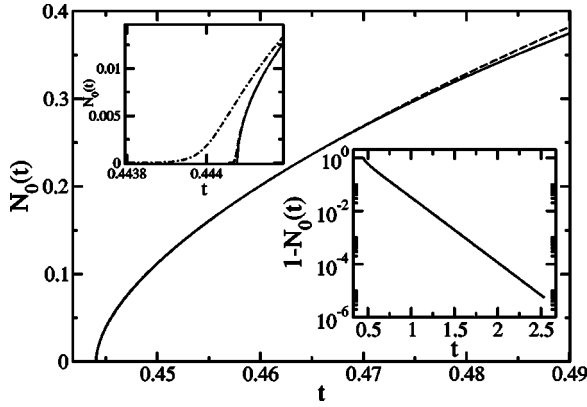
FIG. 1. We plot $N_0(t)$ for small times (solid line). This is compared to $N_0(t)^{\text{theory}} \times [1 + a(t - t_{coll})^b]$ (dashed line), where $N_0(t)^{\text{theory}}$ is given by Eq. (81) with $\mu = 8.389\,171\,47\ldots$, and $a \approx 1.7$ and $b \approx 0.33$ are fitting parameters. Note that the validity range of this fit goes well beyond the estimated t_* with $t_* - t_{coll} \sim T^{D/2} \sim 0.09$. The bottom inset illustrates the exponential decay of $1 - N_0(t) \sim e^{-\lambda t}$. The best fit for λ leads to $\lambda \approx 5.6362$ to be compared to the eigenvalue computed by means of Eq. (86), $\lambda = 5.636\,125\,3\ldots$. Finally, the top inset illustrates the sensitivity of $N_0(t)$ to the space discretization, which introduces an effective cutoff (a factor of 4 between each of the three curves). Note the small time scale. Even the curve corresponding to the coarsest discretization becomes indistinguishable from the others for $t > 0.448$.

$$M(r,t) \approx N_0^{fit}(t) + \frac{\rho_0^{fit}(t)}{3} r^3 + a_5(t) r^5 + a_6(t) r^6 \quad (110)$$

in a region of a few dr, excluding of course $r = 0$. This functional form is fully compatible with the expected expansion for $M(r,t)$, both below ($a_6 = 0$) and above ($a_5 = 0$) t_{coll}. We find that this numerical scheme allows us to cross smoothly the singularity at t_{coll}. An effective cutoff is introduced which effectively depends on dr, and we have checked that the results presented in this section are extremely close to the ones that would be obtained in the ideal limit $dr \to 0$. This is illustrated in Fig. 1, where the smoothing effect of our algorithm is shown to act on a very small time region after t_{coll}. Even more surprisingly, we find that for sufficiently large times (actually very small compared to any physical time scales), our results are essentially independent of dr, even for unreasonably large values of dr. We are thus confident that we have successfully crossed the collapse singularity.

In Fig. 1, we plot $N_0(t)$ for small time which compares well with the universal form of Eq. (81), where $\mu = 8.389\,171\,47\ldots$ has been determined so as to ensure the proper behavior of $S(x)$ for large x (see Sec. V A). We also illustrate the exponential decay of $1 - N_0(t)$, with a rate in perfect agreement with the value of λ extracted from solving numerically the eigenvalue problem of Eq. (86). Finally, we show the effect of the numerical spatial discretization dr near $r = 0$. Satisfactorily enough, the value of $N_0(t)$ is sensitive to the choice of dr only for very small times after the collapse, and we were able to easily reach small enough dr, in order to faithfully reproduce the postcollapse singularity. In Fig. 2, we convincingly illustrate the postcollapse scaling and com-
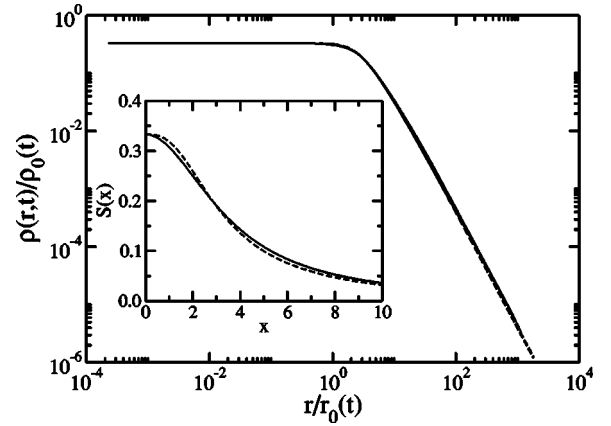

FIG. 2. In the postcollapse regime, we plot $\rho(r,t)/\rho_0(t)$ as a function of the scaling variable $x = r/r_0(t)$. A good data collapse is obtained for central residual densities in the range $10^3 - 10^6$. This is compared to the numerical scaling function computed from Eq. (79) (dashed line). The inset shows the comparison between this postcollapse scaling function (dashed line) and the scaling function below t_{coll} which has been rescaled to have the same value at $x = 0$, preserving the asymptotics: $S(x) = (3 + x^2/4)^{-1}$ [see Eq. (36), solid line]. Note that the postcollapse scaling function is flatter near $x = 0$, as $S(x) - 1/3 \sim x^3$ (in $D = 3$) above t_{coll} instead of $S(x) - 1/3 \sim x^2$, below t_{coll}.

pare the postcollapse scaling function to that obtained analytically below t_{coll} (precollapse). In Fig. 3, we confirm the validity of our perturbative expansion for λ, in the limit of small temperature. We compare the value of c_D extracted from directly solving the full eigenvalue problem to that obtained from Eq. (100), finding perfect agreement. Finally, in
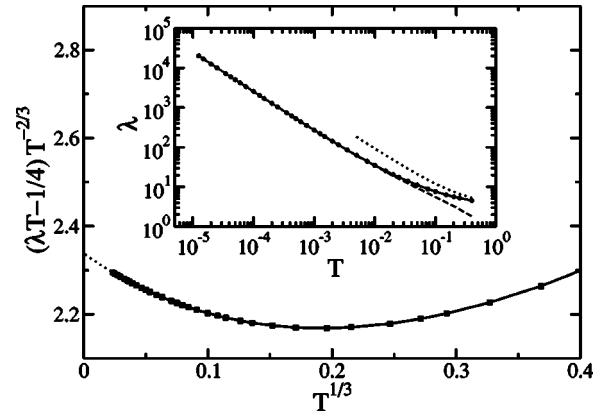

FIG. 3. The main plot represents $\left(\lambda T - \frac{1}{4}\right) T^{-2/3}$ as a function of $T^{1/3}$ (line and squares), which should converge to $c_{D=3} = 2.338\,107\,41\ldots$ for $T \to 0$ according to Eq. (101). We find perfect agreement with this value using a quadratic fit (dotted line). Furthermore, this fit shows that the slope at $T = 0$ is in fact equal to -2 ± 2.10^{-4}, suggesting that the next term to the expansion of Eq. (101) is $\lambda = 1/4T + c_3 T^{-1/3} - 2 + \cdots$, in $D = 3$. In the inset, we plot λ as a function of T up to $T \approx T_c \approx 0.4$. The small-temperature analytical result of Eq. (101) is in very good agreement with the numerical data up to $T \sim 0.03$, whereas the large-T estimate $\lambda(T) = 3 + \frac{9}{10} T^{-1} + \cdots$ is only qualitatively correct in this range of physical temperatures, $T \lesssim T_c$.
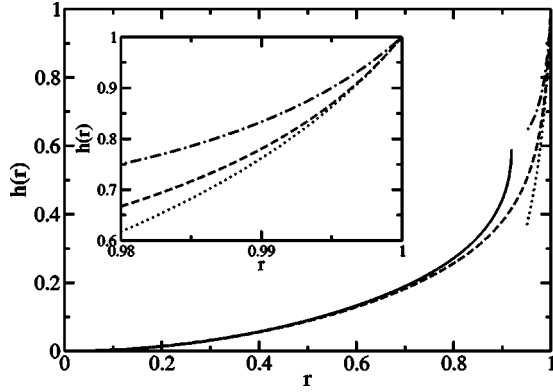
FIG. 4. For $T=0.01$ ($\lambda=35.074\,198\ldots$, $\mu=0.317\,398\,77\ldots$), we plot $h(r)$ computed numerically from Eq. (90) (dashed line) and the theoretical expression of Eq. (92), which is valid for $1-r\gg\mu^2\sim T^{2/3}$ (solid line). We also plot the theoretical expression of z_0 [dash-dotted line; see Eq. (98)] and the next-order perturbation result [dotted line; see Eq. (99)], which are valid in the region $1-r\ll\mu^2\sim T^{2/3}$. The inset is a blowup of the region close to 1. Note how $h(r)$ varies by a quantity of order unity as r varies by a quantity of order $T=0.01$. We have chosen a not too small value for T in order to be able to visualize the two scale regimes in a single figure. Both approximations shown in the inset are getting better as T decreases.

Fig. 4, we compare the numerical value obtained for $h(r)$ to the different analytical estimates given in the preceding section, for $T=0.01$. The two important regions $1-r\ll\mu^2\sim T^{2/3}$ and $1-r\gg\mu^2\sim T^{2/3}$ can be clearly identified.

VII. POSTCOLLAPSE IN THE MICROCANONICAL ENSEMBLE

So far, we have only addressed the postcollapse dynamics in the canonical ensemble. In the microcanonical ensemble, the dynamical equation has to be supplemented with the strict energy conservation condition [see Eq. (24)], which fixes the global temperature $T(t)$. For this model, it was shown in [8,19,20] that below a certain energy (Antonov energy), the system collapses with an apparent scaling associated with $\alpha_{max}\approx2.2$ for intermediate times (when the temperature still increases in a noticeable way) before entering a scaling regime with $\alpha=2$, identical to that obtained in the canonical ensemble. In the limit $t\to t_{coll}$, the temperature and potential energy both seem to converge to a finite value, preserving a constant energy. Closely before the collapse time, the temperature behaves as $T(t_{coll})-T(t)\sim(t_{coll}-t)^\gamma$ with $\gamma\simeq1/2$. This section addresses the $t>t_{coll}$ time period.

Assuming a spherical mass density and after integration by parts, the potential energy W can be rewritten in the form ($D>2$)

$$W(t)=-\frac{1}{2}\int_0^1\frac{M^2(r,t)}{r^{D-1}}dr-\frac{1}{2(D-2)}. \tag{111}$$

We see immediately that as $D-1>1$, the occurrence of a finite mass $N_0(t)\neq0$ concentrated at $r=0$ implies an infinite potential energy, hence an infinite temperature. We thus an-

ticipate that the postcollapse dynamics in the microcanonical ensemble is probably an ill-defined problem. In this extreme regime, let us try to consider the possible flaws of this model in order to describe a consistent dynamics of a reasonable physical self-gravitating system. First, our assumption of uniform temperature is certainly not realistic in a system displaying huge density contrast, and some alternative approaches are needed to incorporate a spatially dependent temperature. This point is certainly crucial and will be addressed in a future work [32]. Furthermore, in this regime, a careful physical analysis predicts that this system of self-gravitating individual particles should lead to the formation of binaries, which is probably beyond the description ability of our essentially mean-field approach. In other words, the system may become intrinsically heterogeneous, which probably cannot be captured by our continuous model. Finally, we can think of other physical effects (degeneracy effects of quantum or dynamical origin, finite-particle-size effects, etc.), preventing the system from reaching arbitrarily large densities. One way to describe such effects consists in introducing a spatial cutoff h or a density cutoff of order h^{-D}. In such a system, the dynamics first follows the precollapse dynamics until the maximum density is approached. Then, the system will ultimately reach a maximum-entropy state that we propose to characterize in a simple manner, as in [33,24].

We propose to describe the final state as a "core-halo" structure, which for simplicity we modelize as a core of radius $h\ll1$ and constant density

$$\rho_{core}=\frac{DN_0}{S_Dh^D}, \tag{112}$$

which mimics a regularized central Dirac peak containing a mass N_0. In the region $h<r\leq1$ stands the halo of constant density,

$$\rho_{halo}=\frac{D(1-N_0)}{S_D(1-h^D)}, \tag{113}$$

containing the rest of the mass. As h is small, we can compute the potential (or total) energy and the entropy, only including the relevant leading terms. We find

$$E=\frac{D}{2}T-\frac{D}{D^2-4}\left[\frac{N_0^2}{h^{D-2}}+1+\frac{D-2}{2}N_0-\frac{D}{2}N_0^2\right]+O(h^2), \tag{114}$$

where the first term is the kinetic energy, whereas the entropy (up to irrelevant constants) reads

$$S=\frac{D}{2}\ln T-N_0\ln\left(\frac{N_0}{h^D}\right)-(1-N_0)\ln(1-N_0)+O(h^D). \tag{115}$$

For a given small value of h, S has a local maximum at $N_0=0$ provided that $E>E_c(h)$, with $\lim_{h\to0}E_c(h)=-D/(D^2-4)$. Below E_c, the sole entropy maximum resides at N_0, satisfying the implicit equation (again in the limit of small h)
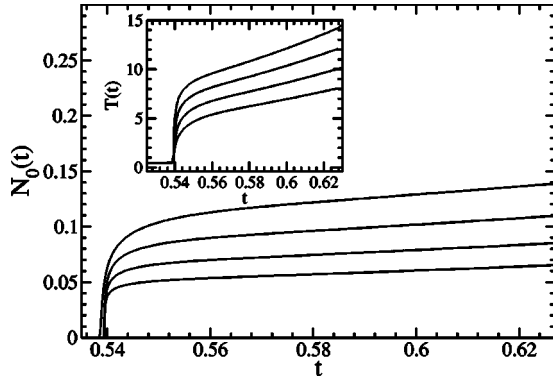
FIG. 5. For $E=-0.45 < E_c \approx -0.335$, we plot $N_0(t)$, for different values of h decreasing by a factor of 2 for each curve from the top one to the bottom one. It is clear that $N_0(t)$ decreases as h decreases. The inset shows the corresponding temperature plots. The temperature $T(t)$ increases as h decreases. Note that in the precollapse regime, the temperature essentially does not depend on h. For the situation considered, it starts from $T(0)=0.1$ and culminates at $T(t_{coll}) \approx 0.5$.

$$N_0 = \frac{D}{\ln\left(\dfrac{N_0}{h^D}\right)} \sim -\frac{1}{\ln h}, \tag{116}$$

where the given asymptotics is quantitatively correct only for extremely small values of h. Hence, we find that the mass included in the core slowly *decreases* with core size h [24], resulting in an effective singularity $\rho(\mathbf{r})=-(1/\ln r)\delta^D(\mathbf{r})$. Meanwhile, the temperature diverges as

$$T \sim -\frac{2}{D}W \sim \frac{2}{D^2-4}\frac{1}{h^{D-2}\ln^2 h} \tag{117}$$

and leads rapidly and efficiently to a uniform halo.

In order to relate this result to our actual system, we perform microcanonical postcollapse simulations using the same regularization scheme as in the canonical case in order to describe the evolution of $N_0(t)$. In addition to this, we also need to regularize the potential energy which is strictly infinite (as well as T) when $N_0 \neq 0$. Consistently with the previous discussion, we introduce a numerical cutoff h by defining

$$W(t) = -\frac{1}{2}\int_h^1 \frac{M^2(r,t)}{r^{D-1}}dr - \frac{1}{2(D-2)}. \tag{118}$$

In Fig. 5, we plot $N_0(t)$ and $T(t)$ for different values of the cutoff h. Contrary to the canonical case, the postcollapse dynamics is strongly h dependent. We see that in conformity with our result of Eq. (116), the central mass N_0 clearly decreases as $h \to 0$. Therefore, in the microcanonical case, the physical picture is that when the collapse time t_{coll} is reached, the temperature increases rapidly, which leads to the rapid homogenization of the system except for a dense and small core, whose mass $N_0 \sim \ln^{-1} T$ is a decreasing function of the maximum temperature reached. This central structure with weak mass and huge binding energy is similar to a "binary star" structure in stellar dynamics. Binary formation is the physical process that arrests core collapse in globular clusters [34]. This is also the end point of our simple microcanonical Brownian model.

VIII. CONCLUSION

In this paper, we have investigated the postcollapse dynamics of a gas of self-gravitating Brownian particles in canonical and microcanonical ensembles. Our results also apply to the chemotactic aggregation of bacterial populations in biology. At the collapse time t_{coll}, the system develops a singular density profile scaling as $\rho \sim r^{-2}$. However, the "central singularity contains no mass," the temperature does not diverge, and the entropy and free energy are finite [8,19,20]. Since this profile is not a maximum entropy (respectively, a minimum free energy) state or a stationary solution of the Smoluchowski-Poisson system, the collapse continues after t_{coll}. This solves the apparent paradox reported in [24].

In the canonical ensemble, mass accretes progressively at the center of the system and a Dirac peak forms by swallowing the surrounding particles. Eventually, the Dirac peak contains all the mass. This structure has an infinite free energy $F=E-TS \to -\infty$ simply because its binding energy is infinite. This is therefore the most probable structure in canonical ensemble [9,10,24]. In the microcanonical ensemble, the maximum-entropy state (at fixed mass and energy) consists of a single binary embedded in a hot halo [23,2,19]. This is precisely what we see in our numerical simulations. The temperature increases dramatically above t_{coll} (resulting in an almost uniform halo) although the mass contained in the core is weak (but finite). We note the "spectacular" fact that almost all the gravitational energy resides in a binarylike core with negligible mass. A similar phenomenon is observed in stellar dynamics for globular clusters having experienced core collapse [1]. This shows that the microcanonical Smoluchowski-Poisson system shares some common properties with kinetic equations usually considered in stellar dynamics (Landau-Fokker-Planck equations), despite its greater simplicity. Clearly, a major drawback of our microcanonical model is to assume that the temperature uniformizes instantaneously, implying an infinite thermal conductivity. We shall relax this simplification in a future work [32]. However, the present study is one of the first dynamical studies showing the formation of Dirac peaks and binarylike structures in systems with gravitational interaction.

Our Brownian model is based on the existence of a gaseous medium that generates a friction force. This situation exists in certain astrophysical models such as the transport of dust particles in the solar nebula [12]. Dust particles are submitted to Stokes or Epstein drag. It is clear that when the concentration of particles is important (prior to planetesimal formation), self-gravity has to be taken into account. Thus, our system of self-gravitating Brownian particles could be connected to this astrophysical situation. We just mention this as a possible astrophysical application because it is not our present main motivation to make a precise model of dust-gas-gravity coupling in protoplanetary disks. However, this problem could be considered in future works.

APPENDIX: BROWNIAN PARTICLE AROUND A "BLACK HOLE"

We consider the Brownian motion of a particle subject to the gravitational force $-GM\mathbf{r}/r^3$ created by a central mass M ("black hole"). We assume that when the particle comes at $r=0$, it is captured by the central mass. We denote by $W(\mathbf{r},t)$ the density probability of finding the particle in $\mathbf{r}$ at time t. It is solution of the Fokker-Planck equation

$$\frac{\partial W}{\partial t} = \boldsymbol{\nabla} \cdot \left(T \boldsymbol{\nabla} W + W \frac{\mathbf{r}}{r^3} \right), \tag{A1}$$

where we have set $G=M=R=\xi=1$. Let $W(r,t)$ denote a spherically symmetric solution of Eq. (A1) satisfying the boundary conditions

$$T\frac{\partial W}{\partial r}(1,t) + W(1,t) = 0, \tag{A2}$$

$$W(r,0) = \frac{\delta(r-r_0)}{4\pi r_0^2}. \tag{A3}$$

We call

$$\mathbf{J} = -\left(T \boldsymbol{\nabla} W + W \frac{\mathbf{r}}{r^3} \right) \tag{A4}$$

the current of probability; i.e., $\mathbf{J}dS\mathbf{n}$ gives the probability that the particle crosses an element of surface dS between t and $t+dt$ ($\mathbf{n}$ is a unit vector normal to the element of surface under consideration).

We introduce the probability $p(r_0,t)dt$ that a particle located initially between r_0 and r_0+dr_0 arrives for the first time at $r=0$ between t and $t+dt$. We have

$$p(r_0,t) = -\int_{R_\epsilon} \mathbf{J} \cdot d\mathbf{S} = 4\pi\epsilon^2 \left(T\frac{\partial W}{\partial r} + \frac{W}{r^2} \right)_\epsilon = 4\pi W(0,t), \tag{A5}$$

where R_ϵ is a ball of radius $\epsilon \to 0$. The total probability that the particle initially between r_0 and r_0+dr_0 has reached the center of the system between 0 and t is thus

$$Q(r_0,t) = \int_0^t p(r_0,t')dt'. \tag{A6}$$

Finally, we average $Q(r_0,t)$ over an appropriate range of initial positions in order to get the expectation $Q(t)$ that the particle has been captured at time t.

With the change of variables

$$W = \psi e^{1/2Tr}, \tag{A7}$$

we can transform the Fokker-Planck equation (A1) into a Schrödinger equation (in imaginary time) of the form

$$\frac{\partial \psi}{\partial t} = T\Delta\psi - \frac{1}{4Tr^4}\psi. \tag{A8}$$

A separation of the variables can be effected by the substitution

$$\psi = \phi(r)e^{-\lambda t}. \tag{A9}$$

This transformation reduces the Schrödinger equation to a second-order ordinary differential equation

$$\phi'' + \frac{2}{r}\phi' + \left(\frac{\lambda}{T} - \frac{1}{4T^2 r^4} \right)\phi = 0, \tag{A10}$$

with the boundary condition

$$\phi'(1) + \frac{1}{2T}\phi(1) = 0. \tag{A11}$$

We note λ_n the eigenvalues and ϕ_n the corresponding eigenfunctions. Since the Schrödinger operator $H=\Delta-1/4T^2 r^4$ is Hermitian, the eigenfunctions form a complete set of orthogonal functions for the scalar product

$$\langle fg \rangle = \int_0^1 f(r)g(r)4\pi r^2 dr. \tag{A12}$$

The system can be furthermore normalized—i.e., $\langle \phi_n \phi_m \rangle = \delta_{nm}$. Any function $f(r)$ satisfying the boundary condition (A11) can be expanded on this basis as

$$f(r) = \sum_n \langle f\phi_n \rangle \phi_n. \tag{A13}$$

In particular,

$$\frac{\delta(r-r_0)}{4\pi r_0^2} = \sum_n \phi_n(r_0)\phi_n(r). \tag{A14}$$

The general solution of the problem (A1) and (A2) can be expressed in the form

$$W(r,t) = \sum_n A_n e^{-\lambda_n t} e^{1/2Tr}\phi_n(r), \tag{A15}$$

where the coefficients A_n are determined by the initial conditions (A3), using the expansion (A4) for the δ function. We get

$$W(r,t) = e^{(1/2T)(1/r-1/r_0)}\sum_n e^{-\lambda_n t}\phi_n(r_0)\phi_n(r). \tag{A16}$$

From this expression, we obtain

$$p(r_0,t) = 4\pi e^{-1/2Tr_0}\sum_n e^{-\lambda_n t}\phi_n(r_0)\lim_{r\to 0}\left[\phi_n(r)e^{1/2Tr} \right]. \tag{A17}$$

Then, according to Eq. (A6), we have

$$Q(r_0,t) = 4\pi e^{-1/2Tr_0}\sum_n \frac{1-e^{-\lambda_n t}}{\lambda_n}\phi_n(r_0)\lim_{r\to 0}\left[\phi_n(r)e^{1/2Tr} \right]. \tag{A18}$$

Finally, averaging over the initial conditions, the probability that the particle has been captured by the central mass at time t can be expressed as

$$Q(t) = \sum_n Q_n(t), \qquad (A19)$$

where

$$Q_n(t) = B_n(1 - e^{-\lambda_n t}) \qquad (A20)$$

and

$$B_n = 4\pi \frac{1}{\lambda_n} \overline{e^{-1/2Tr_0}\phi_n(r_0)} \lim_{r\to 0} \left[\phi_n(r)e^{1/2Tr}\right]. \qquad (A21)$$

This formally solves the problem. If we consider the large-time limit, we just need to determine the first eigenvalue $\lambda_0(T)$ of the quantum problem. This has been done analytically in Sec. V B in the limits $T\to 0$ and $T\to +\infty$.

Below, we consider again the high-temperature regime where thermal fluctuations prevail over gravity but we do not restrict ourselves to the first eigenvalue. To leading order in the limit $T\to +\infty$, the Fokker-Planck equation (A1) reduces to the pure diffusion equation

$$\frac{\partial W}{\partial t} = T\frac{1}{r^2}\frac{\partial}{\partial r}\left(r^2\frac{\partial W}{\partial r}\right). \qquad (A22)$$

However, for consistency (see Sec. V B), it is necessary to keep the term of order $1/T$ (arising from the gravitational force) in the boundary condition. Hence, we take

$$\frac{\partial W}{\partial r}(1,t) + \frac{1}{T}W(1,t) = 0. \qquad (A23)$$

The general solution of the diffusion equation (A22) with the boundary conditions (A23) and (A3) can be expressed as

$$W(r,t) = \sum_n e^{-\lambda_n t}\phi_n(r_0)\phi_n(r), \qquad (A24)$$

where ϕ is solution of

$$\phi'' + \frac{2}{r}\phi' + \frac{\lambda}{T}\phi = 0, \qquad (A25)$$

$$\phi'(1) + \frac{1}{T}\phi(1) = 0. \qquad (A26)$$

Setting $\phi = \chi/r$, Eqs. (A25) and (A26) become

$$\chi'' + \frac{\lambda}{T}\chi = 0, \qquad (A27)$$

$$\chi'(1) = \left(1 - \frac{1}{T}\right)\chi(1). \qquad (A28)$$

Equation (A27) is readily solved. The eigenvalues can be written $\lambda_n = Tx_n^2(T)$, where $x_n(T)$ are the solutions of the implicit equation

$$\tan(x_n) = \frac{x_n}{1 - 1/2T}. \qquad (A29)$$

The eigenfunctions are

$$\phi_n(r) = A_n\frac{\sin(x_n r)}{r}. \qquad (A30)$$

The general solution of the diffusion equation can thus be written

$$W(r,t) = \frac{1}{rr_0}\sum_{n=0}^{+\infty} e^{-Tx_n^2 t}A_n^2\sin(x_n r)\sin(x_n r_0), \qquad (A31)$$

with

$$A_n^2 = \frac{x_n}{2\pi(x_n - \sin x_n\cos x_n)}. \qquad (A32)$$

If we consider the pure diffusion of a particle in a box, the boundary condition (A26) reduces to $\phi'(1)=0$ and the x_n are solutions of the implicit equation

$$\tan(x_n) = x_n. \qquad (A33)$$

In particular, $x_0=0$. This implies that the probability $W(r,t)$ converges for large times to a *uniform* profile $W(r,+\infty) = 3/4\pi$ which is indeed solution of the diffusion equation in a box. If gravity is taken into account, its first-order effect (in the limit $T\to +\infty$) is to change the boundary condition to Eq. (A26). It is *as if* we had a diffusion across the box [27,12] although the true physical process is a capture by the central mass. The eigenvalues are now determined by Eq. (A29). The $x_{n>1}$ are hardly modified (to first order) with respect to the preceding problem but x_0 is now different from zero. To first order, we find that $x_0^2=3/T$ so that $\lambda_0=3$ in agreement with the result of Sec. V B. We also note that $A_0^2=T/4\pi$ while $A_{n>0}$ are independent on T (to leading order) and given by Eqs. (A32) and (A33).

Using Eqs. (A5) and (A6), the probability that the particle has been captured by the central mass at time t is given by

$$Q(t) = \frac{4\pi}{T}\sum_{n=0}^{+\infty}\frac{1 - e^{-Tx_n^2 t}}{x_n}A_n^2\overline{\frac{\sin(x_n r_0)}{r_0}}. \qquad (A34)$$

If we average over initial conditions with the weight $3r_0^2$ (uniform distribution), we find to leading order in T^{-1} that

$$\overline{\frac{\sin(x_n r_0)}{r_0}} = 0, \text{ for } n > 0, \qquad (A35)$$

$$\overline{\frac{\sin(x_0 r_0)}{r_0}} = x_0. \qquad (A36)$$

Hence, the modes $n>0$ cancel out. Therefore, in the high-temperature regime, the probability of capture is given by

$$Q(t) = 1 - e^{-3t}, \qquad (A37)$$

for all times.

The case $D=2$ can be treated by a similar method. Instead of Eqs. (A31), (A32), and (A29), we get

$$W(r,t) = \sum_{n=0}^{+\infty} e^{-Tx_n^2 t}A_n^2 J_0(x_n r)J_0(x_n r_0), \qquad (A38)$$

$$A_n^2 = \frac{1}{\pi[J_1^2(x_n) + J_0^2(x_n)]}, \tag{A39}$$

$$\frac{x_n J_1(x_n)}{J_0(x_n)} = \frac{1}{T}, \tag{A40}$$

where J_n is the Bessel function of order n. For the pure diffusion process, $x_n = \alpha_{1n}$ are the zeros of J_1. If gravity is taken into account, then $x_{n>1} \simeq \alpha_{1n}$ while $x_0^2 = 2/T$ establishing $\lambda_0 = 2$. The probability that the particle has been captured by the central mass at time t is given by

$$Q(t) = \frac{2\pi}{T} \sum_{n=0}^{+\infty} \frac{1 - e^{-Tx_n^2 t}}{x_n^2} A_n^2 \overline{J_0(x_n r_0)}. \tag{A41}$$

If we average over the initial conditions with a weight $2r_0$ (uniform distribution), we get $\overline{J_0(x_n r_0)} = 0$ if $n > 0$ and $\overline{J_0(x_0 r_0)} = 1$. Therefore, in the high-temperature regime, the probability of capture is given, for all times, by

$$Q(t) = 1 - e^{-2t}. \tag{A42}$$

Finally, for $D = 1$, we obtain

$$W(r,t) = \sum_{n=0}^{+\infty} e^{-Tx_n^2 t} A_n^2 \cos(x_n r)\cos(x_n r_0), \tag{A43}$$

$$A_n^2 = \frac{1}{1 + \sin(2x_n)/2x_n}, \tag{A44}$$

$$x_n \tan(x_n) = \frac{1}{T}. \tag{A45}$$

For the pure diffusion process, $x_n = n\pi$. If gravity is taken into account, then $x_{n>1} \simeq n\pi$ while $x_0^2 = 1/T$ establishing $\lambda_0 = 1$. The probability that the particle has been captured by the central mass at time t is given by

$$Q(t) = \frac{2}{T} \sum_{n=0}^{+\infty} \frac{1 - e^{-Tx_n^2 t}}{x_n^2} A_n^2 \overline{\cos(x_n r_0)}. \tag{A46}$$

If we average over the initial conditions with a weight 1 (uniform distribution), we get $\overline{\cos(x_n r_0)} = 0$ if $n > 0$ and $\overline{\cos(x_0 r_0)} = 1$. Therefore, in the high-temperature regime, the probability of capture is given, for all times, by

$$Q(t) = 1 - e^{-t}. \tag{A47}$$

[1] J. Binney and S. Tremaine, *Galactic Dynamics*, Princeton Series in Astrophysics (Princeton University Press, Princeton, 1987).

[2] T. Padmanabhan, Phys. Rep. **188**, 285 (1990).

[3] R. B. Larson, Mon. Not. R. Astron. Soc. **147**, 323 (1970).

[4] H. Cohn, Astrophys. J. **242**, 765 (1980).

[5] D. Lynden-Bell and P. P. Eggleton, Mon. Not. R. Astron. Soc. **191**, 483 (1980).

[6] C. Lancellotti and M. Kiessling, Astrophys. J. Lett. **549**, L93 (2001).

[7] D. Lynden-Bell and R. Wood, Mon. Not. R. Astron. Soc. **138**, 495 (1968).

[8] P. H. Chavanis, C. Rosier, and C. Sire, Phys. Rev. E **66**, 036105 (2002).

[9] M. Kiessling, J. Stat. Phys. **55**, 203 (1989).

[10] P. H. Chavanis, Astron. Astrophys. **381**, 340 (2002).

[11] P. H. Chavanis, Phys. Rev. E **68**, 036108 (2003).

[12] P. H. Chavanis, Astron. Astrophys. **356**, 1089 (2000).

[13] H. Risken, *The Fokker-Planck Equation* (Springer, New York, 1991).

[14] J. D. Murray, *Mathematical Biology* (Springer, New York, 1991).

[15] E. Keller and L. A. Segel, J. Theor. Biol. **26**, 399 (1970).

[16] R. Robert and J. Sommeria, Phys. Rev. Lett. **69**, 277 (1992).

[17] P. H. Chavanis, J. Sommeria, and R. Robert, Astrophys. J. **471**, 385 (1996).

[18] P. H. Chavanis, in *Dynamics and Thermodynamics of Systems with Long Range Interactions*, edited by T. Dauxois, S. Ruffo, E. Arimondo, and E. Wilkens, Lecture Notes in Physics (Springer, Berlin, 2002), e-print cond-mat/0212223.

[19] C. Sire and P. H. Chavanis, Phys. Rev. E **66**, 046133 (2002).

[20] P. H. Chavanis and C. Sire, Phys. Rev. E **69**, 016116 (2004).

[21] M. V. Penston, Mon. Not. R. Astron. Soc. **144**, 425 (1969).

[22] I. A. Guerra, M. A. Peletier, and J. Williams (unpublished).

[23] V. A. Antonov, Vestn. Leningr. Univ., Ser. 3: Biol. **7**, 135 (1962).

[24] P. H. Chavanis, Phys. Rev. E **65**, 056123 (2002).

[25] N. Martzel and C. Aslangul, J. Phys. A **34**, 11225 (2001).

[26] P. H. Chavanis (unpublished).

[27] S. Chandrasekhar, Astrophys. J. **97**, 255 (1943).

[28] N. G. van Kampen, *Stochastic Processes in Physics and Chemistry* (North-Holland, Amsterdam, 1990).

[29] P. H. Chavanis, P. Laurençot, and M. Lemou, Physica A (to be published), e-print cond-mat/0403610.

[30] P. H. Chavanis, M. Ribot, C. Rosier, and C. Sire (unpublished).

[31] W. Jäger and S. Luckhaus, Trans. Am. Math. Soc. **329**, 819 (1992).

[32] C. Sire and P. H. Chavanis (unpublished).

[33] P. H. Chavanis and J. Sommeria, Mon. Not. R. Astron. Soc. **296**, 569 (1998).

[34] M. Hénon, Ann. Astrophys. **5**, 369 (1961).